

ARTICLE

## Study on Mechanical Behaviour of Al-15Si-10Zn/x ZrO<sub>2</sub> Composites Synthesized by Stir Cast Method

Vijaykumar Chavan<sup>1</sup>, Dayanand M. Goudar<sup>2\*</sup>, Vinay V. Kuppast<sup>1</sup>, Rajashekar V. Kurahatti<sup>1</sup>, Mangalppa M. Naik<sup>3</sup>

<sup>1</sup> Department of Mechanical Engineering, Basaveshwar Engineering College, Bagalkot, 587101, India

<sup>2</sup> Department of Mechanical Engineering, Tontadarya College of Engineering, Gadag, 582101, India

<sup>3</sup> Department of Mechanical Engineering, B.V.V.S Polytechnic, Bagalkot, 587101, India

### ABSTRACT

In this research, the microstructure and mechanical properties of Al-15Si-10Zn-xZrO<sub>2</sub> ( $x = 5, 7$  and  $10$  wt.%) composites synthesized by the stir-casting process have been investigated. The matrix and composite samples were characterized using an X-ray diffraction test (XRD) and their microstructures were studied using optical microscopy and scanning electron microscopy (SEM). The microstructure of different phases was analyzed using energy-dispersive spectroscopy (EDS). The microstructure of the Al-15Si-10Zn/ZrO<sub>2</sub> composites consisted of coarse primary Si, needle-like eutectic Si, and Zn-rich phases, with ZrO<sub>2</sub> reinforcement particles distributed homogeneously in the composites. The micro-hardness and tensile properties of the matrix and composites were determined at room temperature. The results show significant improvements in the micro-hardness and tensile strength of the composites compared to the matrix alloy. The micro-hardness of the stir-cast composites increased by 24%, 44%, and 58% in the 5, 7, and 10 wt% ZrO<sub>2</sub> reinforcement composites, respectively. The ultimate tensile strength (UTS) of the 5, 7, and 10 wt% ZrO<sub>2</sub> composites increased by 17%, 30%, and 44%, respectively, compared to the matrix alloy. The increased content of ZrO<sub>2</sub> resulted in an increase in hardness, ultimate tensile and yield strengths and a decrease in ductility.

**Keywords:** Al-Si-Zn/ZrO<sub>2</sub> composites; Stir-casting; Microstructure; Hardness; Yield strength; Tensile strength; Ductility

#### \*CORRESPONDING AUTHOR:

Dayanand M. Goudar, Department of Mechanical Engineering, Tontadarya College of Engineering, Gadag, 582101, India; Email: dmngoudartce@gmail.com.

#### ARTICLE INFO

Received: 21 August 2023 | Revised: 10 October 2023 | Accepted: 13 October 2023 | Published Online: 15 October 2023

DOI: <https://doi.org/10.30564/jmmr.v6i2.5914>

#### CITATION

Chavan, V., Goudar, D.M., Kuppast, V.V., et al., 2023. Study on Mechanical Behaviour of Al-15Si-10Zn/x ZrO<sub>2</sub> Composites Synthesized by Stir Cast Method. Journal of Metallic Material Research. 6(2): 10-19. DOI: <https://doi.org/10.30564/jmmr.v6i2.5914>

#### COPYRIGHT

Copyright © 2023 by the author(s). Published by Bilingual Publishing Group. This is an open access article under the Creative Commons Attribution-NonCommercial 4.0 International (CC BY-NC 4.0) License. (<https://creativecommons.org/licenses/by-nc/4.0/>).

## 1. Introduction

The demand for high-strength and light materials is increasing due to rapid developments in the automobile and aerospace. Binary aluminum-silicon (Al-Si) alloys with more than 13% Si are the leading commercial cast alloys due to their high wear resistance, high strength-to-weight ratio, low thermal expansion coefficient, good machinability, and good castability<sup>[1]</sup>. Many studies have been carried out on the effect of Si content on the mechanical properties of the hypereutectic Al-Si cast alloys<sup>[2]</sup>. It was observed that the hypereutectic range of binary Al-Si alloy depicts poor mechanical properties. This is due to the microstructure of the hypereutectic Al-Si alloy consisting of coarse polygon with sharp-edged Si and needle eutectic Si particles causing matrix instability and stress concentration at the particle edges<sup>[3]</sup>. Aluminum matrix composites (AMCs), whose properties may be customized by the inclusion of particular reinforcements, are becoming more attractive materials for cutting-edge applications in aerospace and automotive<sup>[4]</sup>. The alloying of a trace amount of zinc (Zn) to the Al-Si alloy results in a decrease in the eutectic needle size and an improvement in the homogeneity of the matrix<sup>[5]</sup>. Dhakar et al.<sup>[6]</sup> reported that the alloying of Zn with the hypereutectic Al-Si alloy results in the formation of high-density precipitates in the microstructure, which significantly results in an increase in tensile strength, wear resistance, and hardness<sup>[7,8]</sup>.

Alloying Zn to the Al-Si alloy enhances strength but decreases elongation because of the accumulation of coarse eutectic phases in the alloy. Because of this, it is impracticable to only increase Zn concentration to improve the material's overall performance<sup>[9]</sup>. AMCs became a high-performance material for application in the aerospace, automotive, transportation, and aerospace industries due to their higher strength, high elastic modulus, and increased wear resistance over typical base metals<sup>[10]</sup>. The different types of carbides and oxides, such as Si<sub>3</sub>N<sub>4</sub>, Bn, SiC, TiC, BiC, Al<sub>2</sub>O<sub>3</sub>, TiB<sub>2</sub>, B<sub>4</sub>C, and ZrO<sub>2</sub>, are being used as reinforcements in aluminum matrix composites<sup>[10]</sup>.

Zirconium dioxide (ZrO<sub>2</sub>), the crystalline oxide of zirconium, also known as zirconium oxide, is a

ceramic element and is widely used as a reinforcing particle for high-temperature applications because of its high melting point (1850 °C) ZrO<sub>2</sub> particles have extremely good tribological properties, high thermal (16.7 W/m-K) conductivity, good specific heat capacity (0.285 J/g-°C) and corrosion resistance<sup>[11]</sup>. Also, the high fracture toughness of ZrO<sub>2</sub> particles decreases in the catastrophic failure of composites<sup>[12]</sup>. It is worth noting that zirconium oxide does not react with aluminum at lower temperatures, which is important in preventing the growth of unwanted brittle reactions at interfaces. Additionally, using reinforced zirconium oxide in aluminum alloys can reduce the risk of catastrophic failure during service conditions. Zircon-reinforced composites are preferred as these composites exhibit relatively high refractoriness and excellent resistance to abrasion, thermal shock, and chemical attack compared to composites reinforced with other reinforcements<sup>[13]</sup>. Song Xiu-an et al.<sup>[14]</sup> studied the new silicon-reinforced Zn-Al alloy in a large composition range, as the Si phase is modified with sodium salt compounds and rare metal oxides. Results show that the effects of sodium salt compounds and rare metal oxides on the silicon phase promote each other, the mechanical properties of silicon-reinforced Zn-Al alloys are improved, and the selected alloy. K.B. Girisha et al.<sup>[15]</sup> found that the composites containing ZrO<sub>2</sub> reinforcement showed improved wear properties and hardness strength. Salimi et al.<sup>[16]</sup> demonstrated that accumulative roll bonding resulted in excellent ZrO<sub>2</sub> particle distribution in the aluminum matrix, leading to enhanced tensile, hardness, and elongation properties. Hajizamani et al.<sup>[17]</sup> also observed increased yield strength, ultimate tensile strength, and compressive strength with the addition of Al<sub>2</sub>O<sub>3</sub>-10% ZrO<sub>2</sub> reinforcement. These findings collectively suggest that the incorporation of ZrO<sub>2</sub> reinforcement in an aluminum matrix composite can enhance its mechanical properties. Muralidharan et al.<sup>[18]</sup> found that the addition of ZrO<sub>2</sub> particles to AA6061 increased the hardness and tensile strength of the composites. Pandiyarajan<sup>[19]</sup> also observed improved hardness and strength in Al6061-grade aluminum alloy composites reinforced with ZrO<sub>2</sub>. Kavitha et al.<sup>[20]</sup> investigated

AA6081 composites reinforced with  $ZrO_2$  and found enhanced mechanical properties, including hardness and compressive strength. Overall, these findings suggest that  $ZrO_2$  reinforcement positively impacts the mechanical properties of aluminum matrix composites.

Rathaur et al. <sup>[21]</sup> focus on the mechanical and structural properties of an Al-7075/Si<sub>3</sub>N<sub>2</sub>/ZrO<sub>2</sub> hybrid composite, showing improved tensile strength, hardness, and wear properties with increasing zirconia reinforcement. Abd-Elaziem et al. <sup>[22]</sup> investigated Zn-Al matrix composites reinforced with alumina, carbon, or steel fibers, demonstrating reduced creep rate, thermal expansion coefficient, and improved impact toughness. Jin Wang et al. <sup>[23]</sup> investigated the silicon particle-reinforced zinc-based composites fabricated using a gravity casting technique with sodium salt as a modifier. The results show that the fabrication technique of Si particle-reinforced Zn-based composites with fine silicon particles distributed uniformly can be obtained, and with the increase in Si content in the alloy, the hardness of the alloy increases, the impact toughness of the alloy decreases, and with the increase of Si content in the alloy, the flowability of the high Al-Zn zinc-based alloy decreases. The stir-casting process is a cost-effective and convenient method for producing Aluminium Matrix Composites (AMCs) <sup>[24]</sup>. Although there have been numerous studies on the wear behavior of Al-based composites, there has been limited research on the mechanical properties of hypereutectic Al-Si-Zn-based composites with  $ZrO_2$  reinforcement. In this research, the stir-casting process was used to synthesize Al-15Si-10Zn matrix composites reinforced with  $ZrO_2$  particles of varying wt.% (5, 7, and 10%).

The main objective of this work was to study the microstructure and investigate the impact of  $ZrO_2$  content on the hardness, yield strength, ultimate tensile strength and ductility of the Al-15Si-10Zn/ $xZrO_2$  ( $x=5, 7$  and  $10$  wt.%) stir-cast composites and compared with the matrix alloy.

**Novelty statement:** Numerous research publications were carried out on the mechanical and wear behavior of  $ZrO_2$  reinforced hypoeutectic Al-Si alloy

with small content of Zinc matrix composites. The present work aim is to study the mechanical behavior of hypereutectic Al-Si-Zinc based on different quantities of  $ZrO_2$  reinforced stir-casted composites. The findings collectively suggest that hypereutectic Al-Si-Zn based matrix composites can be tailored to exhibit desirable mechanical and thermal properties through the addition of  $ZrO_2$  reinforcement and is the potential material for automobile applications parts like piston, cylinder and piston rings etc.

## 2. Experimental procedure

### 2.1 Materials and methods

The base alloy Al-15Si-10Zn was prepared using master alloys in a graphite crucible using electric furnace (**Figure 1a**). The chemical composition of the matrix alloy is displayed in **Table 1**. The matrix alloy was then remelted in an electrical furnace at a temperature of 850 °C and treated with hexachloroethane degassifier tablets and scum powder to remove gases from the melt. After skimming, pre-heated  $ZrO_2$  reinforcement powder with a size ranging between 20 to 50  $\mu$ m and different wt.% (5, 7, and 10%) was added to the melt. The chemical composition of the  $ZrO_2$  reinforcement and composite materials is shown in **Tables 2 and 3**. The mixture was stirred by a mechanical stirrer (**Figure 1b**) at a speed of 400 rpm for 15 minutes to ensure an even distribution of the  $ZrO_2$  particles in the matrix alloy. The mixture was then poured into a pre-heated mold (**Figure 1c**) to prepare casting samples with a diameter of 50 mm and a length of 250 mm (**Figure 1d**). The standard size and image of the tensile test sample (as per ASTM standards) are shown in **Figure 2**.

### 2.2 Metallographic examination

In order to examine the microstructure of the matrix and composites, a sample was prepared using standard grinding and polishing techniques. The surface of the sample was then treated with Keller's reagent. The microstructure was analyzed using an optical microscope (Zeiss) and a scanning electron

**Table 1.** Chemical composition of Al-5Si-10Zn alloy Metal matrix.

Elements	Si	Zn	Fe	Mn	Mg	Sn	Al
Wt.%	15	10	0.112	0.009	0.007	0.008	Bal

**Table 2.** Chemical composition of ZrO<sub>2</sub> reinforced powder (wt %).

Constituent	SiO <sub>2</sub>	TiO <sub>2</sub>	Fe <sub>2</sub> O <sub>3</sub>	ZrO <sub>2</sub>
Wt.%	10	0.112	0.009	Bal

**Table 3.** Chemical composition of Al-5Si-10Zn-x (x=5, 7, 10) ZrO<sub>2</sub> composites.

Composite	Elements wt.%							
	Si	Zn	ZrO <sub>2</sub>	Fe	Mn	Mg	Sn	Al
Al-15Si-10Zn-5ZrO <sub>2</sub>	14.28	10.1	4.95	0.112	0.002	0.004	0.002	Bal
Al-15Si-10Zn-7ZrO <sub>2</sub>	15.12	9.93	7.23	0.141	0.001	0.006	0.002	Bal
Al-15Si-10Zn-10ZrO <sub>2</sub>	14.92			0.163	0.002	0.003	0.002	Bal

microscope (Model: JEOL JSM-6480LV). The chemical compositions of the constituents present in different phases were determined using an energy-dispersive X-ray (EDX) micro-analyzer. The SEM was operated at an acceleration voltage of 10-30 kV. The X-ray diffraction analysis was carried out on a pan analytical Philips system (Model: MCRS 2000-3). This system has a Cu-K $\alpha$  anode ( $\lambda = 0.154065$  nm) and 482 kW sealed tube operated at 160 kV and 20 mA. The step size and step time are 0.01 and 1° respectively. The observed d-values were compared with corresponding peaks given in JCPDS files.

### 2.3 Hardness test

The micro hardness of the matrix alloy and composites were measured using a Vickers hardness testing machine (Model: HV-5, Meta-tech) under the load of 250 g and dwell time of 15 s, in accordance with the standard ASTM E92-17, and the average of 5 readings values was reported.

### 2.4 Tensile test

The standard tensile specimens (**Figure 2**) of the matrix and composites were tested at room temperature by following the ASTM E-8 standard (ASTM, 2000). The typical configuration of a tensile specimen is shown in **Figure 2**. The tensile test was carried out using universal testing machine (Model:

Instron, Strain gauge type, 2630-102) at a cross-head speed of 0.0083 mms<sup>-1</sup> and strain rate of 0.05 min<sup>-1</sup>. The yield strength (YS) was calculated according to the standard 0.2% offset strain. The samples were mounted on two grips and aligned with the load axis. The test data reported was the average of three tests.



**Figure 1.** (a) Melting furnace, (b) mechanical stirrer, (c) steel mold and cylindrical castings.

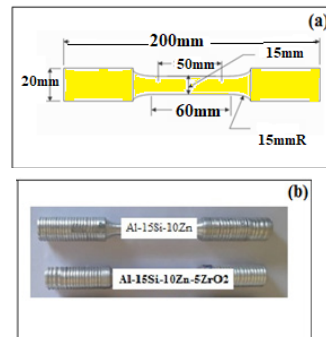


**Figure 2.** (a) Schematic of the tensile test specimen (ASTME8), (b) tensile test specimen.

### 3. Results and discussion

#### 3.1 XRD analysis

**Figure 3** shows the X-ray diffraction pattern of the  $ZrO_2$  reinforcement particulates and composite samples. The XRD pattern of  $ZrO_2$  powder displayed in **Figure 4a** shows clear diffraction peaks at  $2\theta$  values of  $28.2^\circ$ ,  $31.5^\circ$ ,  $38.5^\circ$ ,  $50.1^\circ$ , and  $59.8^\circ$ , which correspond to the  $[-111]$ ,  $[111]$ ,  $[120]$ ,  $[022]$ , and  $[131]$  planes, respectively, of monoclinic  $ZrO_2$ . On the other hand, **Figure 3b** presents the qualitative X-ray diffraction analysis of the composite material. It can be observed that the peaks correspond to reflections of atomic planes belonging to Al, and Si and reflections of crystalline planes of Zn-rich and  $ZrO_2$  phases. The composite exhibits high-intensity peaks of  $\alpha$ -Al and Si and low-intensity peaks of Zn and  $ZrO_2$  phase.

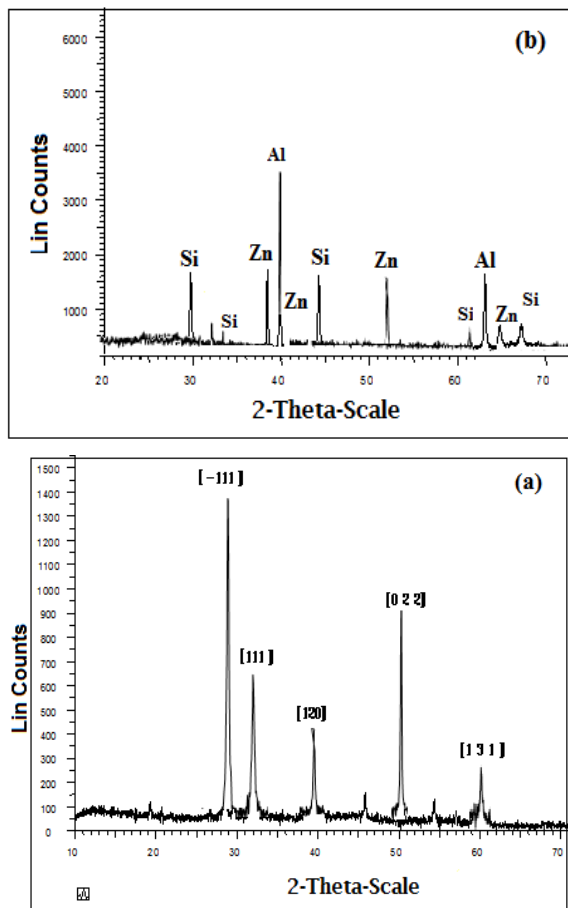


**Figure 3.** Qualitative analysis of XRD pattern (a) matrix and (b) composite material.

#### 3.2 Microstructure study

**Figure 4a** displays an optical micrograph of the Al-15Si-10Zn matrix alloy. It contains coarse polygonal primary Si, needle eutectic Si particles, and dendrite-shaped Zn-rich phases, which are non-uniformly dispersed in the dendrite Al matrix. The formation of blocks of primary Si and needle-like eutectic Si phase is due to the solidification rate of the Al-Si alloy. It is also observed that dendritic Zn-rich phase clusters exist between the eutectic Si and Al-rich phases. **Figures 4b-4d** show the optical microstructure of stir cast composites. Its microstructure mainly consists of primarily consists of coarse and nearly spheroidized primary Si, small size needle form of eutectic Si, Zn-rich phases, and uniformly dispersed  $ZrO_2$  particles in the matrix. It is clearly observed that the distributions of the  $ZrO_2$  are uniform over the entire sample.

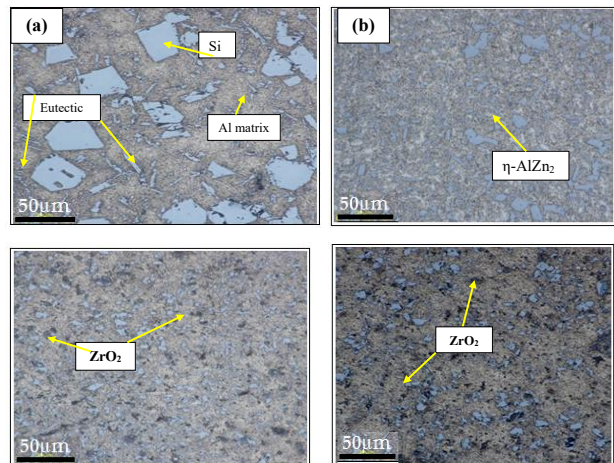


**Figure 4.** Optical micrographs (a) Al-15Si-10Zn alloy, (b) Al-15%Si-10%Zn/5ZrO<sub>2</sub>, (c) Al-15%Si-10% Zn-7%ZrO<sub>2</sub>, and (d) Al-15%Si-10% Zn-10%ZrO<sub>2</sub> composites.

The SEM microstructure of the matrix and composites is shown in **Figure 5**. The SEM microstructure of matrix alloy (**Figure 5a**) mainly consists of Al-rich dendrites, interdendritic Zn-rich phase, needle-like eutectic Si, and block-like Si particles. The addition of Zn causes an increase in coarse Si particles and their segregation in the matrix. Furthermore, the shape of eutectic Si particles changed from needle-like to rounded-like form. The SEM micrographs of Al-Al-15Si-10Zn composites with 5, 7, and 10 %

ZrO<sub>2</sub> particles are shown in **Figures 5b-5d**. It is observed that the ZrO<sub>2</sub> particles are uniform distribution of ZrO<sub>2</sub> particles throughout the matrix. The agglomerated reinforcement (white contrast) particles can be noticed in the composites having a η-AlZn<sub>2</sub> high content of ZrO<sub>2</sub>. From the microscopic image (**Figure 5d**), it is observed that with increasing ZrO<sub>2</sub> content, the agglomeration of ZrO<sub>2</sub> particles in the matrix.

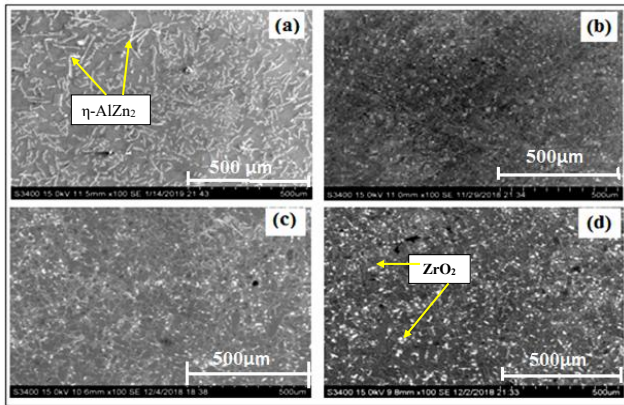


**Figure 5.** SEM microstructure of matrix and stir casted composites (a) Al-15Si-10Zn matrix, (b) Al-15Si-10Zn 5wt.% ZrO<sub>2</sub>, (c) Al-15Si-10Zn-7wt.% ZrO<sub>2</sub>, and (d) Al-15Si-10Zn/10wt.% ZrO<sub>2</sub> composite.

SEM micrograph displaying the point of EDS analysis and the corresponding EDS spectrum of the

Al-15Si-10Zn-7wt.%ZrO<sub>2</sub> composite is presented in **Figure 6**. EDS spots 1, 2, and 3 correspond to the primary Si phase, ZrO<sub>2</sub>, α-Al, and Zn-rich phases, respectively. **Table 4** shows the composition of phases that correspond to the points indicated in **Figure 5**.

### 3.3 Micro-hardness

**Table 5** shows the micro-hardness of the base and composites. The composite materials show high hardness compared to the matrix alloy. The hardness of the composites increased with an increase in ZrO<sub>2</sub> content. The composites have 5, 7 and 10 wt.% ZrO<sub>2</sub> reinforcement shows nearly 29%, 35%, and 66.0% respectively. The high hardness values compared to the matrix alloy. The high hardness of composites is due to increasing ZrO<sub>2</sub> reinforcements, which increase the fraction of hard volume of Si and ZrO<sub>2</sub> phases. This restricts localized deformation of the softer matrix under indentation load. Due to the stir-casting method, the composite exhibits a homogeneous distribution of fine, hard Si and Zn-rich phases. This distribution helps to reduce stress concentration and prevent plastic deformation [24]. The addition of Zn with Al-Si alloy also helps to retain more solute during solidification, leading to solid

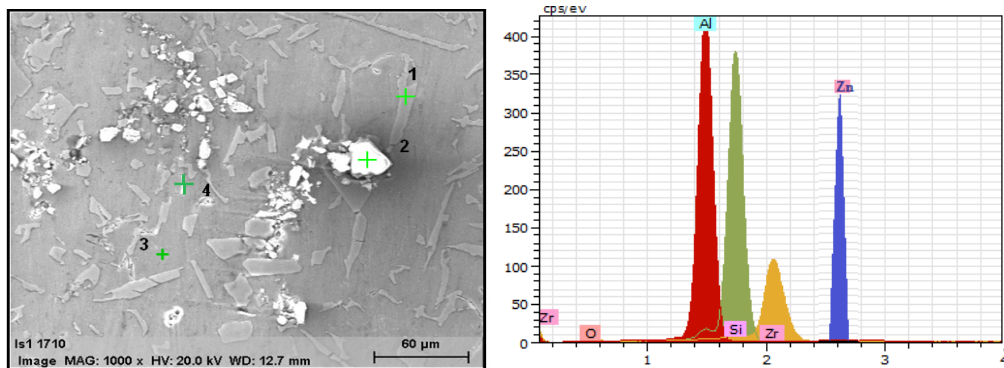


**Figure 6.** (a) SEM/EDS micrograph and (a) EDS spectrum of Al-15Si-10Zn-7wt.%ZrO<sub>2</sub> composite.

**Table 4.** EDS analysis of Al-15Si-10Zn-7wt.%ZrO<sub>2</sub> composite.

Mass (%)					
EDS Spot	O	Al	Si	Zr	Zn
1	0.32	3.50	92.86	3.33	0.00
2	20.46	0.28	0.35	78.91	0.00
3	0.77	92.75	0.37	0.00	6.11
4	0.12	5.67	0.18	0.00	94.12

solution strengthening in the matrix. These factors contribute to the superior hardness of the composite. The high hardness in the composite is also due to the large difference in the thermal expansion coefficients of the  $ZrO_2$  particle and the base alloy. As a result, during the solidification process numerous formation of dislocations at the interface between the  $ZrO_2$  particles and the base. This leads to an increase in resistance to plastic deformation, which is a significant resistance to indentation deformation <sup>[25]</sup>.

**Table 5.** Vickers micro-hardness values of matrix and composites.

Alloy/composite	Micro-hardness $H_v$
Matrix	$65 \pm 3$
5% $ZrO_2$ composite	$88 \pm 5$
7% $ZrO_2$ composite	$92 \pm 4$
10% $ZrO_2$ composite	$88 \pm 5$

### 3.4 Tensile properties

**Table 6** displays the UTS, YS, and ductility of the composites. The results reveal that the UTS and YS of the composite increase with the rise in  $ZrO_2$  wt.%. Compared to the base alloy, the UTS of the 5, 7, and 10 wt%  $ZrO_2$  composites rose by 17%, 30%, and 44% respectively. Increasing the  $ZrO_2$  content results in improved UTS and YS, but ductility decreases with an increase in  $ZrO_2$  wt.%. Hard  $ZrO_2$  and Si particles act as load-bearing elements and lead to high UTS. During tensile loading, the Al-15Si-10Zn matrix transfers the load to hard  $ZrO_2$  and Si particles, increasing the fracture resistance in the matrix. The improved tensile strength is also attributed to the strong interfacial bonding between reinforcement particles and the matrix alloy, which is due to the presence of the Zn-rich phase <sup>[26]</sup>. The yield strength of composites increases noticeably and ranges from 128 to 144 MPa with an increase in  $ZrO_2$  content from 5 to 10 wt.%. The low tensile strength in the matrix owing to the presence of the block-like primary Si with sharp edges, eutectic Si in the form of needles, and flake-like Zn-rich intermetallic on create stress concentrations and become the sites where cracks start to form <sup>[27]</sup>. When a fracture occurs in an alloy, it can spread quickly along

the eutectic and Zn rich secondary phases. The stir casted composites have a more even distribution of hard  $ZrO_2$  particles, nearly spheroidized primary Si, eutectic Si and Zn rich secondary phases, resulting in higher hardness, UTS and YTS. The presence of the Zn-rich strengthening phase, primary Si eutectic phase, and the uniform dispersed  $ZrO_2$  particles have an obstruction caused by the progress of dislocations when the material is subjected to an external load. The increase in the volume percentage of  $ZrO_2$  particles, which act as stress concentrators, results in a reduction in composite ductility.

**Table 6.** Tensile properties of matrix alloy and composites.

Base alloy/Composite	YS (MPa)	UTS (MPa)	Elongation (%)
Base alloy	$115 \pm 6$	$144 \pm 5$	$8 \pm 1.2$
Al-15Si-10Zn/5wt.% $ZrO_2$	$127 \pm 4$	$165 \pm 4$	$4.5 \pm 0.7$
Al-10Zn-5Si/7wt.% $ZrO_2$	$139 \pm 4$	$187 \pm 5$	$4.1 \pm 0.4$
Al10Zn-5Si/10wt.% $ZrO_2$	$144 \pm 7$	$207 \pm 7$	$3.1 \pm 0.34$

### 4. Conclusions

In this study, the hypereutectic Al-15Si-10Zn- $ZrO_2$  composite with reinforcement varying of (5, 7 and 10 wt.%)  $ZrO_2$  material using stir-cast method has been developed. The effect of Zn influence and variation of  $ZrO_2$  quantity on the hardness and mechanical properties of stir-cast hypereutectic Al-Si-Zn composites were studied and compared to the matrix alloy. The study results are summarized below.

- The Al-15%Si-10Zn matrix alloy has a microstructure that consists of primary Si in block-like shapes, eutectic Si in needle-like shapes, and non-uniformly distributed Zn-rich phases in the dendrite  $\alpha$ -Al matrix. The stir cast composites have a homogeneous distribution of  $ZrO_2$  reinforcement particles in the Al matrix.
- The addition of  $ZrO_2$  to the composite resulted in a significant increase in micro-hardness. Specifically, the composite containing 10 wt.%

ZrO<sub>2</sub> displayed approximately 66% higher hardness compared to the matrix alloy.

- The combination of an Al-Si-Zn alloy and reinforced zirconium oxide produces a material with superior mechanical properties. The ultimate tensile strength of composites containing 5%, 7%, and 10% ZrO<sub>2</sub> increased by 17%, 30%, and 44%, respectively, when compared with the matrix alloy. The increase in ZrO<sub>2</sub> content led to a higher hardness and yield strength, while a decrease in ductility.
- The higher hardness and higher mechanical strength of the hypereutectic Al-Si-Zn/ZrO<sub>2</sub> composite can be useful materials for automobile and aerospace applications.

## Author Contributions

Vijaykumar Chavan: Experimental data analysis and drafting.

Dayanand M.Goudar: Literature search, editing, review.

Vinay V. Kuppast: Conceptualization, data curtail.

Rajashekar V.Kurahatti: Editing and supervision.

Mangalappa M. Naik: Methodology.

## Conflict of Interest

No potential conflict of interest was reported by the author(s).

## Data Availability

Not applicable.

## Funding

Not applicable.

## Acknowledgement

The authors gratefully acknowledge the financial support received for this work from Vision Group on Science and Technology (VGST), Government of Karnataka, Bengaluru under the scheme VGST/

K-FIST (LEVEL-I).

## References

- [1] Alshmri, F., 2013. Lightweight material: Aluminium high silicon alloys in the automotive industry. *Advanced Materials Research*. 774, 1271-1276.
- [2] Bogdanoff, T., Seifeddine, S., Dahle, A.K., 2016. The effect of Si content on microstructure and mechanical properties of Al-Si alloy. *La Metallurgia Italiana*. 108(6), 65-69.
- [3] Kaiser, M.S., Sabbir, S.H., Kabir, M.S., et al., 2018. Study of mechanical and wear behaviour of hyper-eutectic Al-Si automotive alloy through Fe, Ni and Cr addition. *Materials Research*. 21(4), 1-8.  
DOI: <https://doi.org/10.1590/1980-5373-MR-2017-1096>
- [4] Ujah, C.O., Kallon, D.V.V., 2022. Trends in aluminium matrix composite development. *Crystals*. 12(10), 1357.  
DOI: <https://doi.org/10.3390/cryst12101357>
- [5] Lee, P.P., Savaskan, T., Laufer, E., 1987. Wear resistance and microstructure of Zn-Al-Si and Zn-Al-Cu alloys. *Wear*. 117(1), 79-89.  
DOI: [https://doi.org/10.1016/0043-1648\(87\)90245-6](https://doi.org/10.1016/0043-1648(87)90245-6)
- [6] Dhakar, P., Kumar, S., Manani, S., et al., 2022. Effect of Zn content on microstructure and properties of hypoeutectic and near-eutectic Al-Si alloys. *IOP Conference Series: Materials Science and Engineering*. 1248(1), 012020.  
DOI: <https://doi.org/10.1088/1757-899X/1248/1/012020>
- [7] Sonker, P.K., Singh, T.J., Yadav, N.P., 2023. Experimental research and effect on mechanical and wear properties of aluminium based composites reinforced with Zn/SiC particles. *Discover Materials*. 3(1), 1-11.  
DOI: <https://doi.org/10.1007/s43939-023-00045-7>
- [8] Savaşkan, T., Hekimoğlu, A.P., 2014. Microstructure and mechanical properties of Zn-15Al-based ternary and quaternary alloys. *Materials Science and Engineering: A*. 603, 52-57.  
DOI: <https://doi.org/10.1016/j.msea.2014.02.047>



- [9] Jiang, H., Xing, H., Xu, Z., et al., 2023. Effect of Zn content and Sc, Zr addition on microstructure and mechanical properties of Al-Zn-Mg-Cu alloys. *Journal of Alloys and Compounds*. 947, 169246.  
DOI: <https://doi.org/10.1016/j.jallcom.2023.169246>
- [10] Harichandran, R., Selvakumar, N., 2016. Effect of nano/micro B<sub>4</sub>C particles on the mechanical properties of aluminium metal matrix composites fabricated by ultrasonic cavitation-assisted solidification process. *Archives of Civil and Mechanical Engineering*. 16, 147-158.  
DOI: <https://doi.org/10.1016/j.acme.2015.07.001>
- [11] Patil, I.S., Rao, S.S., Herbert, M.A., et al., 2022. Experimental investigation and optimisation of mechanical and microstructure behaviour of stir cast and hot-pressed Al-12.5% Si-ZrO<sub>2</sub> composites: Taguchi and super ranking concept. *Advances in Materials and Processing Technologies*. 8(3), 2576-2602.  
DOI: <https://doi.org/10.1080/2374068X.2021.1927648>
- [12] De Aza, A.H., Chevalier, J., Fantozzi, G., et al., 2002. Crack growth resistance of alumina, zirconia and zirconia toughened alumina ceramics for joint prostheses. *Biomaterials*. 23(3), 937-945.  
DOI: [https://doi.org/10.1016/s0142-9612\(01\)00206-x](https://doi.org/10.1016/s0142-9612(01)00206-x)
- [13] Kumar, A., Rana, R.S., Purohit, R., et al., 2022. Metallographic study and sliding wear optimization of nano Si<sub>3</sub>N<sub>4</sub> reinforced high-strength Al metal matrix composites. *Lubricants*. 10(9), 202.  
DOI: <https://doi.org/10.3390/lubricants10090202>
- [14] Song, X.A., 2010. Research on new silicon-reinforced Zn-Al alloys. *Foundry Technology*. 31, 731-734.
- [15] Girisha, K.B., Chittappa, H.C., 2013. Preparation, characterization and mechanical properties of Al356.1 aluminium alloy matrix composites reinforced with MgO nanoparticles. *International Journal of Innovative Research in Science, Engineering and Technology*.
- [16] Salimi, A., Borhani, E., Emadoddin, E., 2017. Evaluation of mechanical properties and structure of Al-1100 composite reinforced with ZrO<sub>2</sub> nanoparticles via accumulative Roll-Bonding. *Transactions of the Indian Institute of Metals*. 70, 989-995.  
DOI: <https://doi.org/10.1007/s12666-016-0892-x>
- [17] Hajizamani, M., Baharvandi, H., 2011. Fabrication and studying the mechanical properties of A356 alloy reinforced with Al<sub>2</sub>O<sub>3</sub>-10% vol. ZrO<sub>2</sub> nano-particles through stir casting. *Advances in Materials Physics and Chemistry*. 1(2), 26.  
DOI: <https://doi.org/10.4236/ampc.2011.12005>
- [18] Muralidharan, N., Chockalingam, K., Kalaiselvan, K., et al., 2023. Investigation of ZrO<sub>2</sub> reinforced aluminium metal matrix composites by liquid metallurgy route. *Advances in Materials and Processing Technologies*. 9(2), 593-607.  
DOI: <https://doi.org/10.1080/2374068X.2022.2095132>
- [19] Pandiyarajan, R., Maran, P., Marimuthu, S., et al., 2022. Investigation on mechanical properties of ZrO<sub>2</sub>, C and AA6061 metal matrix composites. *Advances in Materials and Processing Technologies*. 8(sup1), 178-186.  
DOI: <https://doi.org/10.1080/2374068X.2020.1810946>
- [20] Kavithaa, K.R., Prakasha, S., Ravichandranb, M., 2021. Investigations on non-biodegradable zirconium dioxide reinforced aluminium alloy (AA6081) matrix composite developed by using powder metallurgy route. *Digest Journal of Nanomaterials & Biostructures (DJNB)*. 16(3), 877-888.  
DOI: <https://doi.org/10.15251/DJNB.2021.163.877>
- [21] Rathaur, A.S., Katiyar, J.K., Patel, V.K., 2019. Experimental analysis of mechanical and structural properties of hybrid aluminium (7075) matrix composite using stir casting method. *IOP Conference Series: Materials Science and Engineering*. 653(1), 012033.  
DOI: <https://doi.org/10.1088/1757-899X/653/1/012033>
- [22] Abd-Elaziem, W., Liu, J., Ghoniem, N., et al., 2023. Effect of nanoparticles on creep behaviour of metals: A review. *Journal of Materials Research and Technology*. 26, 3025-3053.  
DOI: <https://doi.org/10.1016/j.jmrt.2023.08.068>
- [23] Wang, J., Xie, N. (editors), 2012. Study on the fabrication and mechanical property of silicon

- particle reinforced Zinc-based composites. 2012 2nd International Conference on Consumer Electronics, Communications and Networks (CECNet); 2012 Apr 21-23; Yichang, China. New York: IEEE. p. 1353-1356.  
DOI: <https://doi.org/10.1109/cecnet.2012.6202183>
- [24] Reddy, M.P., Shakoor, R.A., Parande, G., et al., 2017. Enhanced performance of nano-sized SiC reinforced Al metal matrix nanocomposites synthesized through microwave sintering and hot extrusion techniques. *Progress in Natural Science: Materials International*. 27(5), 606-614.  
DOI: <https://doi.org/10.1016/j.pnsc.2017.08.015>
- [25] Sahu, M.K., Sahu, R.K., 2018. Fabrication of aluminum matrix composites by stir casting technique and stirring process parameters optimization. *Advanced casting technologies*. IntechOpen: London.
- [26] Pul, M., 2021. Effect of ZrO<sub>2</sub> quantity on mechanical properties of ZrO<sub>2</sub>-reinforced aluminum composites produced by the vacuum infiltration technique. *Revista de Metalurgia*. 57(2), 1-13.  
DOI: <https://doi.org/10.3989/revmetalm.195>
- [27] Akbari, M.K., Baharvandi, H.R., Shirvanimoghaddam, K., 2015. Tensile and fracture behavior of nano/micro TiB<sub>2</sub> particle reinforced casting A356 aluminum alloy composites. *Materials & Design*. 66, 150-161.  
DOI: <http://dx.doi.org/10.1016/j.matdes.2014.10.048>